A Numerical Study of the Outflow Layer of Tropical Cyclones

JAINN-JONG SHI

Department of Marine, Earth and Atmospheric Sciences, North Carolina State University, Raleigh, North Carolina

SIMON WEI-JEN CHANG

Naval Research Laboratory, Washington, D.C.

SETHU RAMAN

Department of Marine, Earth and Atmospheric Sciences, North Carolina State University, Raleigh, North Carolina

(Manuscript received 3 November 1989, in final form 26 March 1990)

ABSTRACT

The structure and dynamics of the outflow layer of tropical cyclones are studied using a three-dimensional numerical model. Weak and strong tropical cyclones are produced by the numerical model when starting from idealized initial vortices embedded in mean hurricane soundings. The quasi-steady state outflow layers of both the weak and strong tropical cyclones have similar characteristics: 1) the circulations are mainly anticyclonic (except for a small region of cyclonic flow near the center) and highly asymmetric about the center, 2) the outflow layer is dominated by a narrow but elongated outflow jet, which contributes up to 50% of the angular momentum transport, and 3) the air particles in the outflow jet mostly originate from the lower level, following "in-up-and-out" trajectories.

We found that there are secondary circulations around the outflow jet, very much like those associated with midlatitude westerly jet streaks. In the jet entrance region, the secondary circulation is thermally direct. That is, the ascending motion is located on the anticyclonic shear side of the jet, and the descending motion on the cyclonic shear side. There is a radially outward (perpendicular to the jet) flow above the jet and inflow below it. In the jet exit region, the secondary circulation is weaker and reversed in its direction (thermally indirect). The secondary circulations leave pronounced signatures on the relative humidity, potential vorticity, and tropopause height fields. The secondary circulation is more intense in the stronger tropical cyclone (with a stronger outflow jet) than in the weaker tropical cyclone.

The sensitivities to upper-tropospheric forcing of the outflow are tested in numerical experiments with prescribed forcings. It is found that the simulated tropical cyclone intensifies when its upper levels within a radius of approximately 500 km are accelerated and forced to be more divergent. Convection plays a key role in transforming the upper level divergence into low level convergence. In another experiment, additional regions of convection are initiated in the ascending branches of the circum-jet secondary circulations away from the inner region when the outflow jet between the radii of 500 and 1000 km is accelerated. These regions of convection become competitive with the inner core convection and eventually weaken the tropical cyclone. In both experiments, cumulus convection is the major link between the upper-level forcing and tropical cyclone's response.

1. Introduction

The outflow layer of tropical cyclones is generally shallow, anticyclonic, divergent on the synoptic scale, and considerably more asymmetric than the middle and lower layers (Alaka 1961, 1962; Miller 1963; Black and Anthes 1971; Frank 1977; McBride 1981; Merrill 1988a). Except for a small region near the center, the tropical cyclone outflow is normally concentrated in one or two outflow jets (or channels). It is well known that conditions in the low- and mid-tropospheric environment, such as moist instability, high ocean surface temperatures, and 200–850 mb vertical shears can greatly affect the behavior of tropical cyclones. Recently, however, it has been recognized that the outflow layer is also able to control the intensity or even the movement of tropical cyclones. There have been many observational studies (e.g., Riehl 1954; Sadler 1976, 1978; Holland and Merrill 1984; Steranka et al. 1986; Rodgers et al. 1987, 1990; Molinari and Vollaro 1989) which link the behavior of tropical cyclones to the strength and position of upper tropospheric troughs (UTT). Sadler (1976, 1978) showed that, in general, as an UTT aligns vertically with the underlying tropical cyclone, the tropical cyclone weakens. On the other hand, if a tropical cyclone is aligned with an upper tropospheric ridge, it generally intensifies. Rodgers et al. (1990), based on satellite-measured total ozone,

Corresponding author address: Dr. Simon Chang, Department of the Navy, Code 4110, Naval Research Laboratory/Atmospheric Physics Branch, Washington, DC 20375.

suggested that the positioning of upper-level troughs modulated the inner core convection and, therefore, the intensity of some Atlantic hurricanes.

It has been demonstrated that the asymmetric outflow can be responsible for eddy fluxes of angular momentum comparable in magnitude to those of the tropical cyclone's symmetric radial circulation (Pfeffer 1958; Palmen and Riehl 1957; Black and Anthes 1971; Holland 1983; Molinari and Vollaro 1989). Challa and Pfeffer (1980) showed that the angular momentum flux convergence measured from observational data can accelerate the development of a tropical cyclone in an axisymmetric numerical model. On the other hand, Holland and Merrill (1984) argued that as the tropical cyclone's low- and mid-tropospheric cyclonic circulations develop, the storm becomes more inertially stable, and more resistant to environmental forcing at these levels. However, at the outflow level, they believed that the anticyclonic asymmetric flow is more inertially unstable and more responsive to upper-level environmental forcing. It is not difficult to imagine then that a tropical cyclone outflow jet can be accelerated by an approaching upper-level trough and that the tropical cyclone would intensify under such condition as suggested by Sadler (1976, 1978).

The physical process or the chain of events that allows the upper tropospheric forcing to influence the tropical cyclone is, however, less apparent. The kinetic energy budget in Challa and Pfeffer (1980) indicates that with added angular momentum flux the stronger development of their model tropical cyclone is accompanied by an excess of kinetic energy production due to the pressure torque (that is, the work done by the cross-isobaric, radial circulation). It is not clear, however, whether this enhanced radial circulation is a cause or effect of the intensification. Sadler (1978) speculated that the outflow channel, when strengthened, can extend inward to the innner-core convection and serve as the outflow of the inner-core convection and, therefore, enhance the convection. This view is supported by Chen and Gray (1984), who conjunctured that the enhanced outflow can remove more mass and heat from the inner region of the tropical cyclone and maintain the convective instability.

Merrill (1984, 1988b) proposed a different mechanism for the tropical cyclone's intensification under upper-tropospheric forcing. He noted that the outflow jet, similar to the jet streaks in mid- and high-latitudes, has a secondary circulation around it (Palmen and Newton 1969; Uccellini et al. 1984). He argued that as the jet is enhanced or "channeled" by the jet stream associated with the upper-tropospheric trough, the secondary circulation would also be enhanced. This in turn would initiate additional convection in the upward branch of the secondary circulation and intensify the storm. However, a necessary condition for this process is that the upward branch of the secondary circulation is located near the inner region.

These hypotheses of course cannot be substantiated without the knowledge of the detailed structure of the outflow jet. Analysis of observational data on the outflow level on a single-case basis may suffer from the lack of data or poor spatial coverage, whereas, composite data may not give a dynamically consistent structure. A numerical simulation with a three-dimensional (3D) model seems to be an expedient way to obtain a comprehensive description of the tropical cyclone outflow layer. In the following sections 2 and 3, a brief review of the numerical model will be given and the outflow layer structure simulated by the model will be presented. The plausibility of the upper-level forcing changing the behavior of tropical cyclones will be discussed and examined by conducting additional numerical experiments. These results will be presented in section 4.

2. The numerical tropical cyclone model

The tropical cyclone model used in this study is essentially the same as the Naval Research Laboratory (NRL) limited-area numerical model described in Chang et al. (1989). The model is a 3D, hydrostatic, primitive equation, finite difference model with physical parameterizations of the boundary layer and cumulus convection. Model equations and the numerical techniques are documented in detail in Madala et al. (1987). Some modifications are made to accommodate the simulation of an idealized tropical cyclone.

This model uses the Arakawa C grid with a uniform resolution of 0.5 degree in longitude and latitude. There are 141×91 horizontal points in the model, covering a domain from the equator to 45°N in latitude with a width of 70 degrees in longitude from, say, 110°E to 180°. (The model result is independent of the longitudinal domain.) The model domain is assumed to be entirely over the ocean to avoid complications with sea–land contrasts. A variable Coriolis parameter ($f = 2\Omega \sin\Phi$) is used. There are ten σ ($\sigma = p/p_s$) layers in the vertical with equal σ thickness. As in Chang et al. (1989), a constant drag coefficient and constant exchange coefficients for the sensible and latent heats are used. The use of a simple boundary layer parameterization is justified because the structure of the outflow layer should be relatively insensitive to boundary layer formulations. A modified Kuo's cumulus parameterization scheme is used.

All the simulations presented in this paper are carried out with no initial environmental winds. There are no winds along the lateral boundaries throughout the integration. Although the lateral boundaries remain undisturbed due to the large model domain, a damping scheme is used in a five-point boundary zone to reduce any boundary reflection. To avoid the effect of the sea surface temperature (SST) variations, the SST is set at 302.5 K over the entire model domain. The model is initialized with the mean hurricane sounding from

Sheets (1968). The initial vortex is defined by the following function

$$v^{\lambda}(\sigma, r) = v^{\lambda}_{\max} W(\sigma)\left(\frac{r}{r_0}\right) \exp\left\{\frac{1}{b}\left[1 - \left(\frac{r}{r_0}\right)^{b}\right]\right\} \quad (1)$$

where v^{λ} is the tangential velocity relative to the center, r is the radius, $b = 2$ and $r_0 = 240$ km. The vertical structure function $W(\sigma)$ decreases linearly from 1 at $\sigma = 1$ to 0 at $\sigma = 0.4$, so that the outflow can develop in the model instead of being prescribed by the initial wind profile. The initial position of the vortex is set at 22.5°N, 160°E.

In order to simulate the outflow layer of both a strong and a weak tropical cyclone, two values of $v^{\lambda}_{\max}$ are used: 40 m s^{-1} for the strong storm and 20 m s^{-1} for the weak storm. In addition, for the computation of surface moisture flux in the integration the specific humidity at the ocean surface for the case of the strong storm is assumed to be 100% of the saturation specific humidity at SST. A 5% reduction in the surface specific humidity is assumed for the case of the weak storm. A nondivergent, nonlinear balanced initialization is carried out to obtain the initial conditions for the model integration.

3. The structure of the outflow layer

The model is integrated for 120 and 96 hours for the weak and strong cases, respectively. In early hours of integration, initial vortices weaken due to the onset of surface friction and internal diffusion. As the convection becomes organized, the vortices intensify. Finally, a quasi-steady tropical cyclone develops from the initial vortex after about 72 hours in the weak case and 48 hours in the strong case. The quasi-steady strong storm has a central pressure of about 960 mb and a maximum surface wind of 51.5 m s^{-1} (at 57 h). For the weak storm, the central pressure is about 984 mb and the maximum surface wind is 23.2 m s^{-1} (at 76 h). The quasi-steady storms weaken at a very slow rate and have northwest drifts due to the β effect. The centers of both the strong and weak storms have moved northwest from their initial positions at a speed approximately 3 m s^{-1}.

a. General structure

The outflow is the strongest at the 150 mb level for both storms. This is probably because that the tropopause in the initial sounding is at 150 mb and the convective heating stops there. As shown in Figs. 1 and 2, the outflow is anticyclonic (except for a small area near the center) and covers a larger area than the cyclonic circulation in the lower and middle troposphere. As shown by the isotachs in Figs. 3 and 4, the outflow is dominated by a single jet in each storm. The maximum speed in the outflow reaches 54.4 m s^{-1} in the strong case and 33.6 m s^{-1} in the weak case. In both cases, the jet is ~3000 km long and very narrow with an e-folding half-width of ~200 km. In the direction perpendicular to the jet, there is very strong anticyclonic shear along the jet core facing the storm center and strong cyclonic shear facing away from the center. In both strong and weak storms, the single jet starts from a position north of the central cyclonic circulation (the entrance region), where the large Coriolis parameter causes the strongest inertial acceleration. In a supplementary experiment where a tropical cyclone is embedded in a zonal flow with westerlies to the north

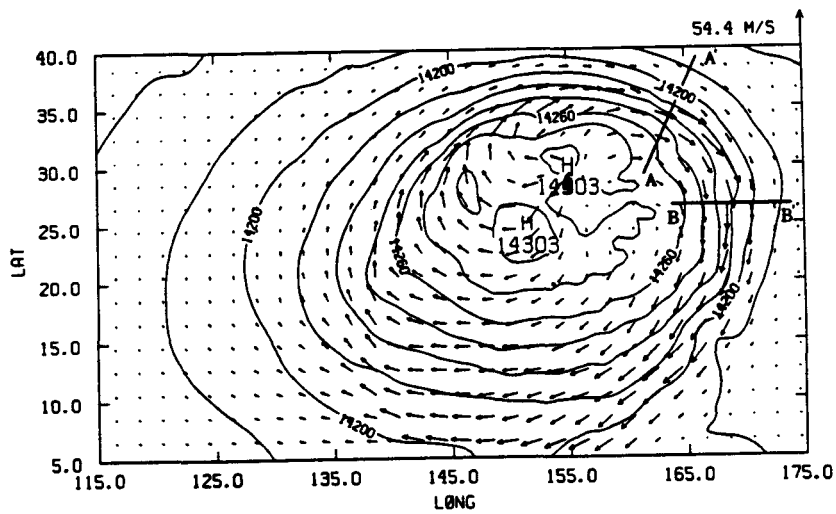

FIG. 1. Geopontential height field (with 15 gpm intervals) and wind vectors at 150 mb level for the strong control case at 72 h. The maximum vector is plotted at the upper-right corner. The location of the surface minimum pressure center is denoted by the hurricane symbol. Note locations of cross sections AA' in entrance region and BB' in exit region. Cross-sectional analyses will be presented in Figs. 5 and 6.

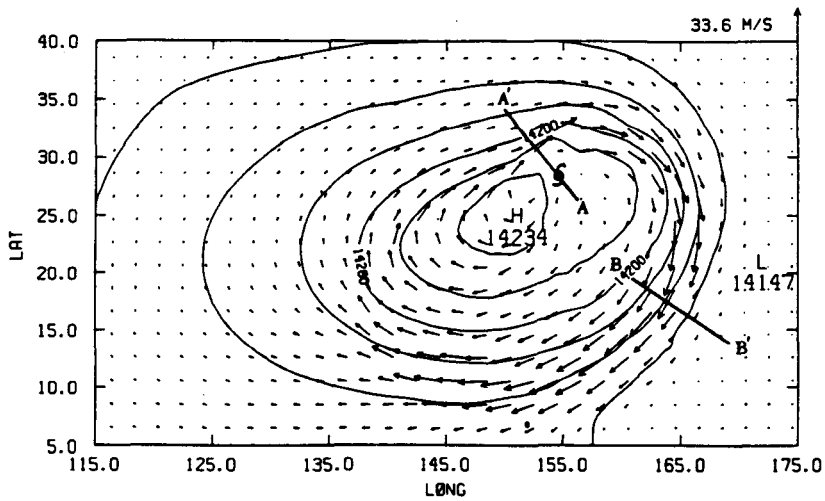

FIG. 2. As in Fig. 1 except for the weak control case at 96 h.

and easterlies to the south of the storm, two jets are formed, in agreement with the result of Ooyama's (1987) single layer model.

As indicated by the isotachs, the section of the jet between the jet maximum (~10° to the east of the storm center) and the exit region (~20° to the south and southwest of the storm center) is more diffused with diminishing horizontal shears. Comparing the two storms, the jet of the stronger storm is of higher speed, wider and located farther away from the center. In all, the characteristics of these two simulated jets are very similar to those observed (Black and Anthes 1971; Sadler 1976; Merrill 1988a).

b. Secondary circulation

Figures 5 and 6 show the normal (in isotachs) and tangential wind components (in vectors) for the cross sections AA′ in the entrance and BB′ in the exit region between the levels of 30 and 300 mb. The normal wind component shows that the jet is very shallow, and confined between 100 and 250 mb, with very strong surrounding horizontal as well as vertical shears. The tangential components of the wind indicate that there are circum-jet secondary circulations, similar to those associated with mid- and high-latitude jet streams (Palmen and Newton 1969; Uccellini et al. 1984). In the entrance region of the outflow jet, the direction of the secondary circulation is such that there is an ascending branch on the anticyclonic shear side (facing toward the center) and a descending branch on the cyclonic shear side (away from the cyclone center). It also has an outward branch above the jet and an inward branch below the jet. Because of the warm core and general warmer inner region, the secondary circulation is thermally direct in the entrance region. In the exit region,

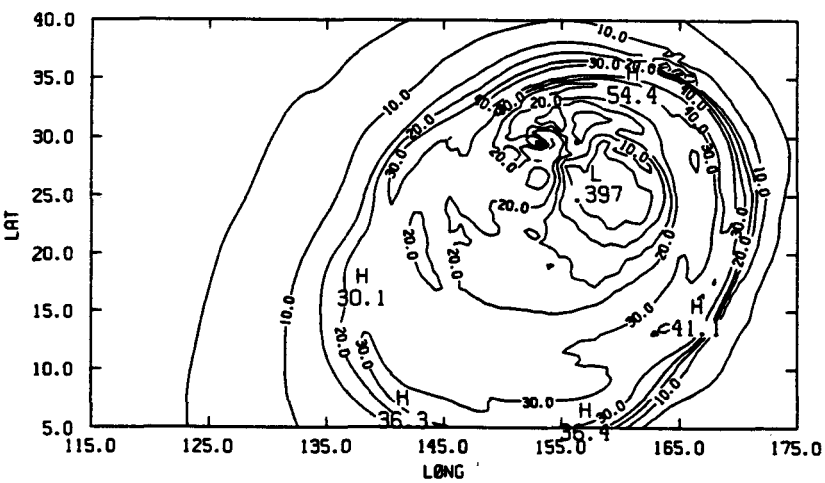

FIG. 3. Isotachs with intervals of 10 m s^{-1} at 150 mb for the strong case at 72 h.

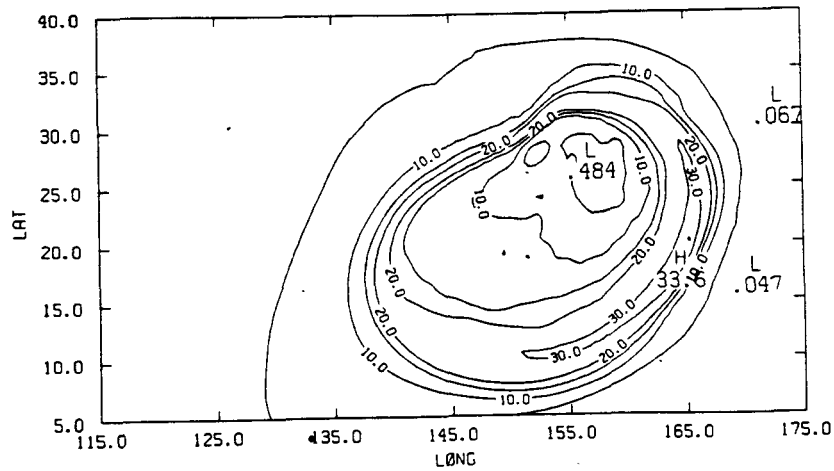

FIG. 4. As in Fig. 3 except for the weak case at 96 h.

the direction of the secondary circulation is reversed (thermally indirect). The upward branch is located on the cyclonic shear side of the jet instead, and the downward branch is located on the anticyclonic shear side of the jet. However, the thermally indirect secondary circulation in the exit region is much weaker and more diffuse than its thermally direct counterpart in the entrance region.

Comparing the maximum vertical and horizontal vectors (shown at the corners of Figs. 5 and 6), it is also apparent that the secondary circulation associated with the stronger jet is stronger than its counterpart for the weaker jet. The existence of the secondary circulation around the outflow jet is crucial for Merrill's (1984) hypothesis that the upper-tropospheric forcing can influence the strength of tropical cyclones through the secondary circulation.

c. *Relative humidity and potential vorticity*

Figures 5 and 6 show the structure of the secondary circulation at a snapshot. To further illustrate that the secondary circulation is a persistent feature associated with the outflow jet, we now discuss the distribution of the relative humidity and potential vorticity at the outflow level. Because there is no significant condensation at the outflow level, the relative humidity (RH) field at the 150 mb level of both the weak and strong storms (shown in Fig. 7) is mainly a manifestation of the transport process, reflecting several important fea-

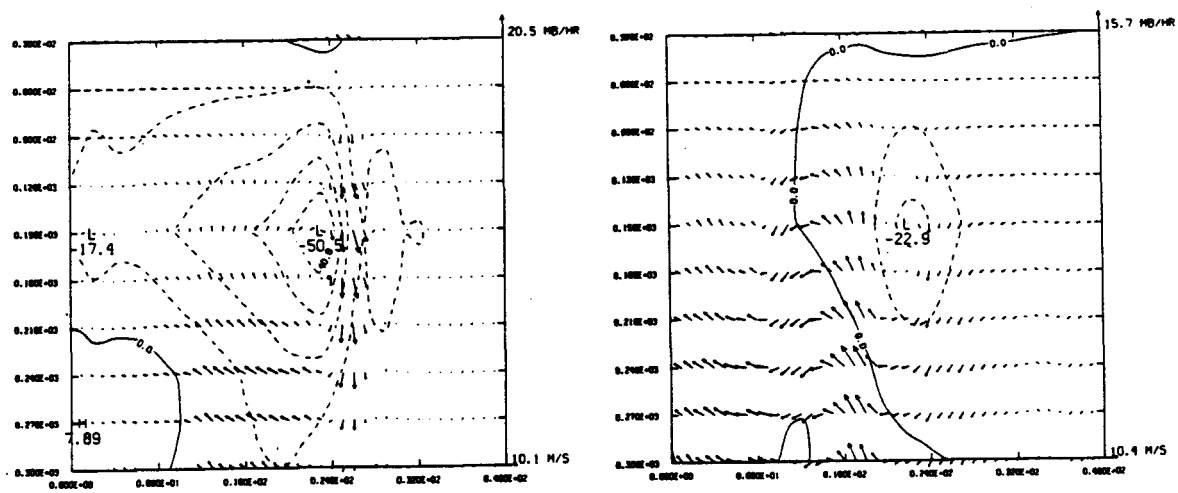

FIG. 5. The wind speed perpendicular (shown by isotachs with negative numbers denoting a wind direction outward from the plot) and tangential (shown by vectors) to the cross section AA′ in the jet entrance region (shown in Figs. 1 and 2) of (a) the strong case at 72 h and (b) the weak case at 96 h. The vectors are formed by horizontal winds in m s^{-1} and vertical velocities in mb h^{-1}. The maximum horizontal and vertical velocity component are plotted at the lower and upper right corners, respectively.

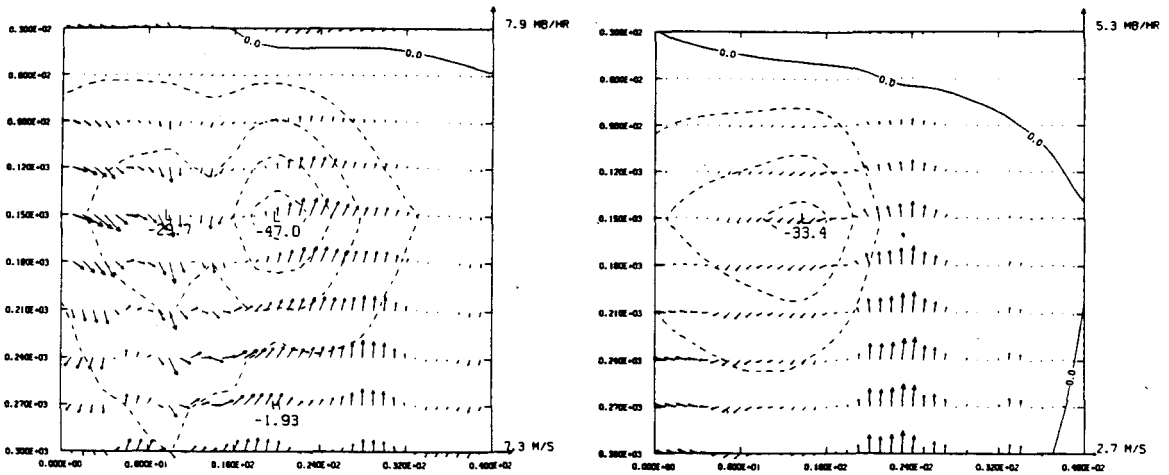

FIG. 6. As in Fig. 5, except for the jet exit region for cross section BB'.

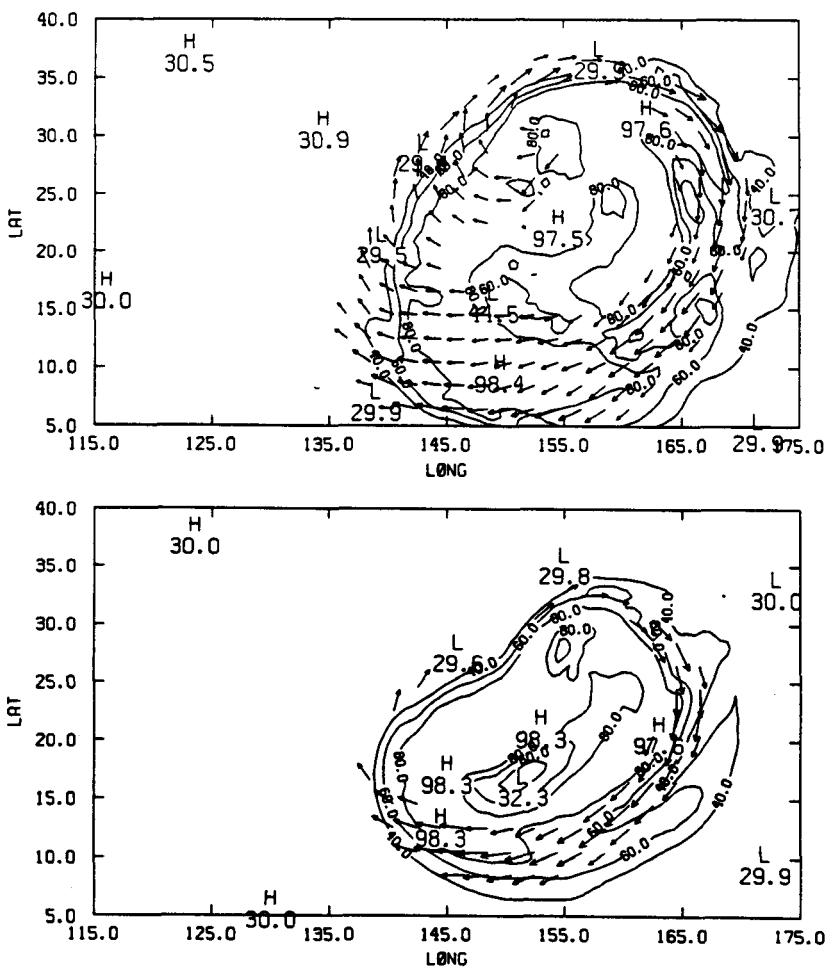

FIG. 7. The 150 mb RH field and the wind vectors >20 m s^{-1} for (a) the strong case at 62 h and (b) the weak case at 96 h.

tures of the outflow momentum field. In general, on the tropical cyclone scale, there is a wet canopy of RH > 80%, with higher values of RH to the south of the storm center. The storm center, in spite of the coarse horizontal resolution, is represented by a drier region of RH < 80% embedded in the wet canopy. There is a very sharp RH gradient in the direction perpendicular to the outflow jet. In the jet entrance region, the RH is >80% on the anticyclonic shear side of the jet, coinciding with the ascending branch of the secondary circulation. On the other hand, the RH is <40% on the cyclonic shear side of the jet due to the descending motion there. This confirms the existence of a steady secondary circulation around the jet.

South of 25°N along the jet core, the secondary circulation reverses direction, and an increase of RH to >60% occurs downwind of the cyclonic shear side of the jet, indicative of the rising motion there. There is a sharp and narrow dry tongue between 25°N, 170°E and 15°N, 160°E (in Fig. 7b, and a similar dry tongue in Fig. 7a), due to the downwind transport by the jet of dry air that originated in the downward branch of the thermally direct secondary circulation. Because the thermally indirect secondary circulation is weaker than the thermally direct one, the RH gradient normal to the jet in the exit region is also weaker as compared to the entrance region. There is a dry region located near 15°N, 150°E in the weak case (and similar dry region in the strong case), probably formed by the downward branch of the thermally indirect secondary circulation and general subsidence of the tropical cyclone.

The potential vorticity (PV), defined as

$$\mathrm{PV} = \frac{1}{\theta}(\zeta + f)\left(\frac{\delta\theta}{\delta p}\right) \qquad (2)$$

where the vorticity $\zeta = \delta v/\delta x - \delta u/\delta y$ is computed on pressure surfaces, is conserved in adiabatic processes (Hoskins et al. 1985). In general, in an undisturbed atmosphere the PV is high in the stratosphere due to the high static stability and low in the troposphere. Therefore, in studying mid- and high-latitude storms, the PV can sometimes be used as a tracer for stratospheric air. A value of 2×10^{-7} mb^{-1} s^{-1} is commonly chosen as the lower limit for stratospheric air (Kuo and Reed 1988; Rodgers et al. 1990). In tropical cyclones, the generation of PV due to latent heating may become important and the PV may not be conserved as well as in mid- and high-latitude systems. However, at the 150 mb outflow level where the latent heating is negligible, the PV may still be a good indicator of general rising and sinking motions, especially outside of the inner convective region.

Figure 8 shows the pressure levels at which the PV = 2×10^{-7} mb^{-1} s^{-1}. In other words, it is the "tropopause" as defined by the PV. Except for the high values near the storm center due to the "eye" effect, there are significant variations of the tropopause heights near the outflow jet. In general, the tropopause is higher (low pressure values) on the anitcyclonic side of the jet, extending from the entrance region downstream, and is lower (high pressure values) on the cyclonic side of the jet. The effects of the secondary circulation of the outflow jet on the spatial distribution of the tropopause are also discussed in cross-sectional plots by Rodgers et al. (1990, Fig. 5).

d. Angular momentum

The outflow plays an important role in the maintenance of the angular momentum balance of tropical cyclones (Palmen and Riehl 1957; Pfeffer 1958; Anthes 1974). An angular momentum budget is calculated

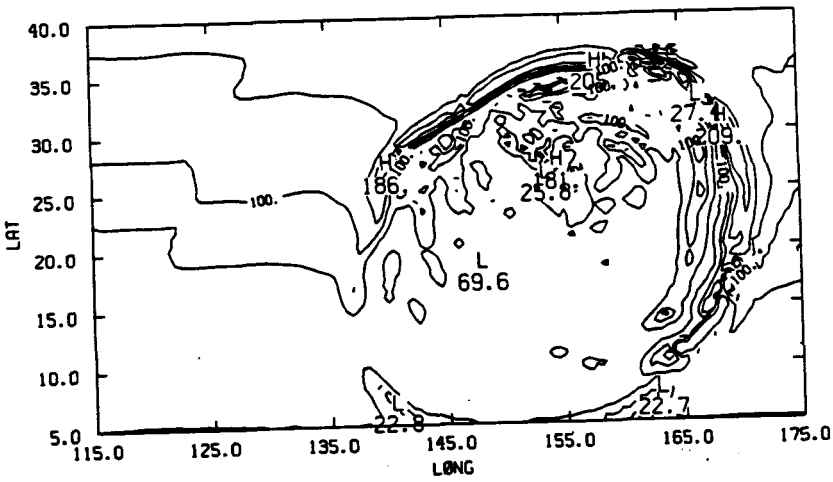

FIG. 8. A plane view of the pressure surface where PV = 2×10^{-7} mb^{-1} s^{-1} for the strong case. This PV value is sometimes used to define the tropopause in midlatitudes.

for the simulated tropical cyclones based on the angular momentum budget equation of Anthes (1974):

$$\frac{\delta M}{\delta t} = -2\pi \int_{h_1}^{h_2} \int_{r_0}^{r_1} r^2 \rho(z)(\langle f \rangle \langle u \rangle + \langle f'u' \rangle) dr dz - 2\pi \int_{h_1}^{h_2} [r_1 \rho(z)(\langle m \rangle \langle u \rangle)_{r_1} - r_0 \rho(z)(\langle m \rangle \langle u \rangle)_{r_0}] dz - 2\pi \int_{h_1}^{h_2} [r_1 \rho(z)(\langle m'u' \rangle)_{r_1} - r_0 \rho(z)(\langle m'u' \rangle)_{r_0}] dz - 2\pi \int_{r_0}^{r_1} r[(\rho \langle m \rangle \langle w \rangle)_{h_2} - (\rho \langle m \rangle \langle w \rangle)_{h_1}] dr - 2\pi \int_{r_0}^{r_1} r[(\rho \langle m'w' \rangle)_{h_2} - (\rho \langle m'w' \rangle)_{h_1}] dr, \quad (3)$$

where u and v are the radial and tangential velocities in cylindrical coordinates, respectively, r is the radius from the center as determined by the lowest surface pressure, and $m = rv$. In the above equation, $\langle\ \rangle$ represents an azimuthal mean and $(\ )'$ denotes a deviation from the mean. Vertical integrations are carried out between the geopotential heights of h_1 = 13 700 gpm and h_2 = 14 700 gpm, encompassing most of the outflow. In (3), the first term on the rhs denotes the mean and eddy Coriolis torque, the second and the third terms denote the horizontal convergences of mean and eddy angular momentum fluxes, respectively. And finally, the fourth and fifth terms represent the vertical convergence of mean and eddy angular momentum fluxes, respectively. To evaluate the values of these terms, model results are linearly interpolated to the cylindrical–pressure coordinates.

Table 1 shows the values of each term in (3) for the simulated strong tropical cyclone at 72 h and the weak tropical cyclone at 96 h. For comparison, observed values for mean tropical storms in Palmen and Riehl (1957) and Pfeffer (1958) are also listed. Our model tropical cyclones are larger in size than the mean storm and therefore the 666 km used as the outer radius of the outflow in observational studies is not appropriate for our model results. Instead, we use radii of 1000 and 1500 km as the outer boundaries for the weak and strong model tropical cyclones, respectively.

Table 1 shows that the values of various terms in (3) evaluated from the modeled tropical cyclones compare reasonably with the observed, considering that the simulated strong tropical cyclone is twice as energetic in terms of horizontal fluxes and Coriolis torque as the mean storm in Palmen and Newton (1969). The angular momentum balance in both simulated and observed tropical cyclones is basically maintained by the Coriolis torque and horizontal transports. Both model and observations show that the contribution by the horizontal eddy momentum flux convergence is in general ~50% of the mean momentum flux convergence, except for the outer region of the model weak storm where the eddy flux is larger than mean flux. Although the single outflow jet in the modeled tropical cyclone cannot account for all of the eddy angular momentum, harmonic decompositions at several radii indicate that the azimuthal wavenumber one has more than 70% of the total eddy angular momentum. The importance of the eddy term again underscores the dominance of the outflow jet in the outflow layer. Note that the vertical momentum fluxes in Palmen and Newton (1957) contain unaccounted-for residuals.

e. *Trajectories*

Trajectories were generated by releasing trace particles at the initial time and tracing them in an attempt

TABLE 1. Model and empirical angular momentum budgets in the upper layer of tropical cyclones. Units are in 10^{22} g cm^{-2} s^{-2}.

Storm	Radius (km)	Coriolis torque	Horizontal flux		Vertical flux	
			Mean	Eddy	Mean	Eddy
Mean Storm (Palmen and Newton 1957)	0–333	−48.0	−20.0	8.0	40.0	20.0
	333–666	−143.0	76.0	23.0	—	44.0
Mean storm (Pfeffer 1958)	222–444	−54.0	46.0	20.0	5.0	—
	444–666	−78.0	−11.0	13.0	−4.0	—
Model (weak)	0–300	−4.3	3.5	−0.7	−0.3	—
	300–1000	−47.6	13.4	35.1	1.1	−0.4
Model (strong)	0–300	−20.2	−4.7	−5.0	7.3	−0.4
	300–1500	−287.1	159.8	79.7	0.5	−6.9

to find the origins of air particles in the outflow layer. A total of 206 trace particles are released at the initial time of the simulated weak tropical cyclone at the 150, 500 and 950 mb levels, and evenly distributed around six concentric rings with respect to the initial vortex center at radii of 20, 100, 300, 500, 1000 and 1500 km. For the weak tropical cyclone, the radius of 20 km is in the "eye," radii of 100 and 300 km are within the inner convective region, 500 km is in the intermediate region, and 1000 and 1500 km are at the outskirts of the tropical cyclone. The pressure levels of 150, 500 and 950 mb are roughly in the outflow, nondivergent, and inflow levels, respectively, of the model tropical cyclone. The position of each particle is calculated by an Euler-backward integration, for which linear interpolations are used to obtain the three dimensional velocity components. Particle positions are stored every three model time steps for trajectory plotting.

Figure 9 shows the trajectories at 96 h formed by some of the 206 particles. The trajectories depict a commonly accepted cyclone scale circulation of an idealized tropical cyclone. There is a cyclonic convergent flow in the low levels, strong upward and cyclonic circulation in the inner region, and a divergent anticyclonic outflow at high altitudes. These trajectories are in general similar to those in Anthes (1972) except that our model domain is larger, which allows a well-defined outflow structure. Upon close examination of particle positions and additional trajectory plots (not shown), the following interesting observations can be made:

(i) Most particles released at 500 and 950 mb at radii of 300 and 500 km are caught in the inner region of convection and transported to the outflow level.

(ii) Most particles released at or transported into the inner region of the outflow level are transported away from the inner region by the outflow jet. The trajectories are very close together in the entrance region and become more diffused in the exit region. There is a general sinking in the outflow jet, for most particles are at 100–150 mb in the jet entrance region but descend to 300 mb in the exit region.

(iii) Particles released at or transported into small radii at low levels (A and B in Fig. 9) are trapped in low levels inside the radius of the maximum updraft. These trapped particles move toward the northwest as the center drifts toward northwest due to the β effect.

4. Response to upper-tropospheric forcing

As discussed in the Introduction, there seems to be at least two ostensibly different mechanisms for the upper troposphere to influence the behavior of tropical

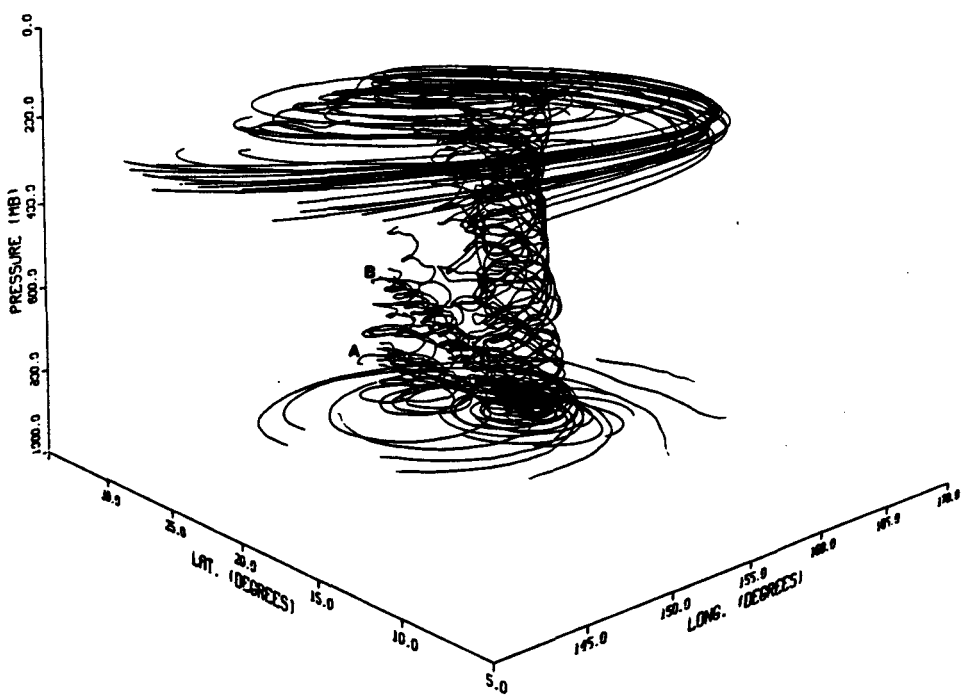

FIG. 9. Trajectories formed by particles released at various radii and pressure levels at $t = 0$. Most particles that reach the outflow level are transported outward by the outflow jet. Most particles released at radii of 20 km (A) and 100 km (B) are "trapped" inside the radius of the maximum wind and only rise slowly and drift toward the NW.

cyclones. The first possible mechanism, postulated by Challa and Pfeffer (1980), Molinari and Vollaro (1989) and others, is that the inner circulation of tropical cyclones can be spun up by an influx of eddy angular momentum when the outflow of tropical cyclones is modified by upper-tropospheric ridge/trough systems. The second mechanism, as proposed by McBride (1981) and others, asserts that when the outflow jet is accelerated by an upper-tropopsheric ridge/trough system, the enhanced secondary circulation can initiate additional deep convection in the inner region, and, thus intensity the tropical cyclone. It has been demonstrated in the previous section that there is indeed a secondary circulation associated with the outflow jet of the simulated tropical cyclones. It is also shown that a stronger secondary circulation associated with the stronger jet. It is thus conceivable that as the outflow jet is accelerated, the secondary circulation will become stronger and may eventually trigger the deep convection that may affect the storm's intensity. It is difficult, however, to completely separate the two mechanisms.

Two different numerical experiments have been conducted to investigate the behavior of the model tropical cyclone in response to the modification of the outflow layer. In these experiments, various parts of the outflow layer are artificially accelerated by a nudging method, i.e., additional tendency terms are added to the momentum equations in the x- and y-direction. The tendency terms are of the form:

$$\frac{\delta p_s u}{\delta t} = \cdots + \lambda p_s(u_0 - u),$$

$$\frac{\delta p_s v}{\delta t} = \cdots + \lambda p_s(v_0 - v), \qquad (4)$$

where the time scale $\lambda = f/2$. Values of $2u(t)$ and $2v(t)$ are chosen for u_0 and v_0 in (4) to get the desired acceleration. Although the extra terms can force an exponential growth of the momentum field, the model's diffusion terms have damping effects which slow down the growth and the numerical experiments are terminated within finite periods of time. Note here both the rotational and irrotational components of the wind are accelerated.

It is not the purpose of this paper to theorize how and/or what part of the tropical cyclone is accelerated under certain upper tropospheric forcings. The cause of such acceleration, may it be accomplished by the approach of an upper level ridge/trough system or by angular momentum transport is outside the scope of this paper. Instead, our purpose is to study the response of the tropical cyclone to the acceleration of a certain part of the troposphere.

a. Accelerating the inner region

In Expt. 1, the inner region in the upper-troposphere of the tropical cyclone is spun up. Specifically, the tendency terms in (4) are applied to all model grid points between 150 and 450 mb within a 5° lat. radius from the center of the storm, as determined from the minimum sea level pressure. This variational experiment is carried out from 72 h for the weak control case. As the tropical cyclone moves toward northwest, the area subjected to the acceleration also moves. This experiment is conducted to simulate the situation when the entire upper part of the inner tropical cyclone is accelerated. As shown by Fig. 10, the central pressure of Expt. 1 deviates gradually from the control experiment after 72 h, becoming more intense and reaching approximately 976 mb at 105 h, 10 mb deeper than the control. The maximum surface wind at this time in Expt. 1 is approximately 22 m s^{-1} as compared with 17 m s^{-1} in the control.

In this experiment, the upper-tropospheric winds in the inner region of the model tropical cyclone are all accelerated and there could be two direct—but not completely separable—dynamic responses to this added forcing. First, the cyclonic circulation that exists in the inner region is spun up. This would decrease the warm core, destabilize the inner region, promote inner-core convection, and eventually lead to the intensification (Gray 1979). However, cumulus convection in the model is likely to quickly stabilize the additional convectively unstable lapse rate and renders the isolation of the effect from the model results very difficult. But as it will be discussed, the cumulus convection plays a important role in tropical cyclone's response to upper-level forcing.

The second response is caused by the breakdown of the quasi-gradient balance of the outflow layer as the result of the forcing. Consider the gradient balance of

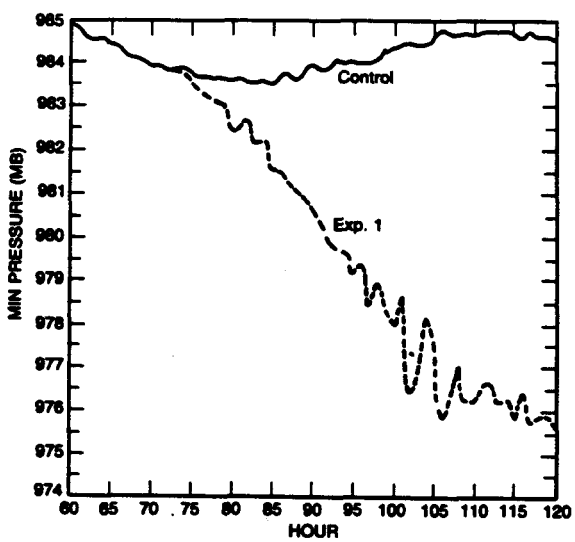

FIG. 10 Variations of the central pressure of the control (weak) and Expt. 1.

$$\frac{1}{\rho}\frac{\delta p}{\delta r} = \left(f + \frac{v}{r}\right)v \qquad (5)$$

where r is the radius and v, the tangential velocity. At very small radii where the circulation is cyclonic (positive v), a supergradient circulation causes divergence. At larger radii but within the forced region of radius of 5° lat (where the winds are anticyclonic), the centrifugal acceleration of a 20 m s^{-1} wind is at least no smaller in magnitude than the Coriolis acceleration (no matter whether the winds are cyclonic or anticyclonic). A supergradient condition then still causes a divergence. Therefore, the forced acceleration in Expt. 1 creates a mean divergence of the outflow layers within the radius of 5° lat. The eddy flux of angular momentum exerted on the upper levels also creates a cyclonic torque and divergence (Eliassen 1952; Challa and Pfeffer 1989). The divergence at the outflow level requires a compensating rising motion and convergence at lower levels for mass continuity. It is unclear what the effect may be if the convergence occurs immediately under the outflow level. However, if the compensating convergence occurs at low levels, the increased convergence would replenish the system with marine boundary layer air of high equivalent potential temperature and could intensify the tropical cyclone. To examine the vertical extent to which the tropical cyclone responds to the upper-level forced divergence, we computed the mass divergence at 96 h with a 10° × 10° box centered around the storm. As shown in Fig. 11, the upper-level mass divergence is approximately 11 × 10^{12} g s^{-1} in Expt. 1, almost twice as strong as the control. The convergence in Expt. 1 is stronger than the control at all levels below σ = 0.45. In the boundary layer, the mass convergence of Expt. 1 is also twice that of the control, similar to the difference between developing and nondeveloping tropical storms (Gray 1979).

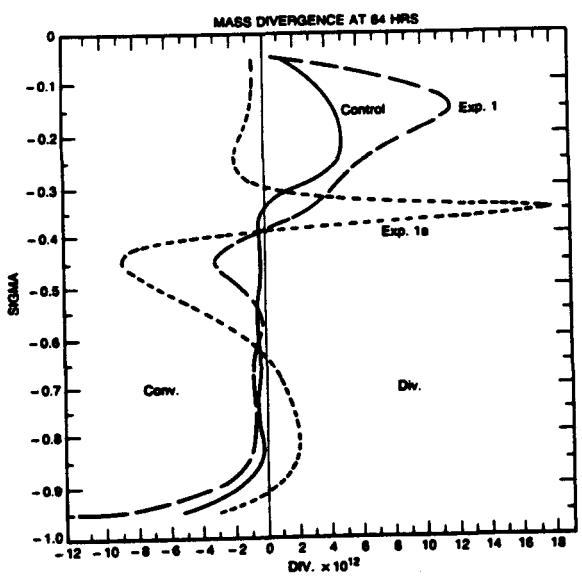

FIG. 11. The vertical distribution of mass divergence/convergence in a 10° long × 10° lat box centered around the storm for the weak control case, Expt. 1, and a supplementary experiment (Expt. 1a) in which latent heating is suppressed.

In the supplementary numerical experiment, Expt. 1 is duplicated except that the cumulus convection is suppressed. The vertical distribution of the mass divergence for this supplementary experiment clearly shows that compensating convergence does not extend to low levels. These results suggest that the deep cumulus convection is a key factor coupling the upper-level dynamics with the low levels.

In summary, results from this experiment seem to support the hypothesis that the tropical cyclone can be modified by the upper-tropospheric forcing. The forced spinup of the inner region of the tropical cyclone creates a supergradient condition in the outflow layer, which in turn results in an upper-level divergence. The cumulus convection helps to produce a compensating convergence in the low level and, thus, the tropical cyclone intensifies.

b. Acceleration of the outflow jet

In the second numerical experiment (Expt. 2), the upper level momentum field is forced as in Expt. 1, except that the forced region is restricted to be between the radii of 5° and 10° from the center and only where the wind speed exceeds 20 m s^{-1}. In fact, the forced region in this experiment is restricted to the jet core located from the northeast to the east relative to the center and between σ = 0.1 to 0.3. The experiment starts from the 48 h of the strong case, which is used as the control for comparison. Accelerations of the radial wind and the tangential wind in the forced region in this experiment have different effects on the mass divergence. Because the circulation in the forced region is divergent, the acceleration in the radial direction causes divergence. The forced anticyclonic acceleration of the jet at the radii of 5° ~ 10°, however, would decrease the inertia term in (5), $fv + v^2/r$, and cause a convergence toward the inner region (in other words, the magnitude of the Coriolis force is larger than the centrifugal force). This experiment differs from those in Challa and Pfeffer (1980, 1989) in that the acceleration due to eddy momentum in their experiments is exerted on all points in their model. In addition, the eddy momentum flux convergence in their experiments results in a cyclonic torque causing divergence at large radii, while in this experiment the acceleration of the jet results in a net anticyclonic torque causing convergence beyond the radius of about 5° lat.

At 96 h, the maximum speed in the outflow jet has increased almost twofold to ~90 m s^{-1}. It is interesting to note that the mass divergence at the outflow level at 72 h (Table 2) changes only slightly from the control

TABLE 2. Mass divergence at $\sigma = 0.15$ for control and Expt. 2 at 72 h. Units are 10^{12} g s^{-1}.

Experiment	5 × 5° box	10 × 10° box
Control experiment	39	39
Expt. 2	34	46

for both the 5 × 5° and the 10 × 10° boxes, as compared with the twofold increase in Expt. 1 (Fig. 11). The small decrease of the divergence for the 5 × 5° box is due to the converging effect of the supergradient jet discussed previously. The increased divergence for the larger 10 × 10° box is due to the forced acceleration of the divergent component of the jet. One may infer from this that the intensity of the tropical cyclone would remain relatively unchanged. However, the central pressure at 96 h is 5 mb higher than the control. An examination of the distribution of the convective heating suggests that the convection induced by the accelerated jet away from the core region appears to *weaken* the tropical cyclone. Figure 12 shows the 24 h for 48–72 h accumulated precipitation amount for the control, and two 12 hourly accumulated precipitation amounts for 48–60 h and 60–72 h for Expt. 2. It is clear that additional precipitation of up to 3.8 cm has been produced on the anticyclonic shear side of the entrance region of the jet in the first 12 h of the experiment. The convection is associated with the upward branch of the direct secondary circulation of the jet, which strengthens because of the acceleration of the jet. By 72 h, the region of the additional precipitation has extended upstream (as suggested by Sadler, 1978) and downstream of the jet, but mainly stays with the upward branch of the circum-jet secondary circulation (i.e., the anticyclonic shear side in the jet entrance region and the cyclonic shear side in the jet exit region). The precipitation over the central region in this experiment is less than the control. The convection away from the core associated with the accelerated jet apparently becomes competitive with the inner core convection and, thus, weakens the tropical cyclone.

It has been observed that Hurricane Florence of 1988 in the Gulf of Mexico may have had a significant interaction with an approaching westerly trough resulting in the explosive development of convection near the outflow jet, which grew even stronger than the inner-core convection. An observational study on this phenomenon is currently ongoing and the result will be reported in the near future. Although other factors may have affected the intensification and decay of Hurricane Florence, the numerical simulation presented here may be of relevance to Florence's behavior.

5. Summary and conclusions

Numerical simulations of idealized tropical cyclones with special emphasis on the outflow layer have been conducted. Results show that the anticyclonic outflow is strongest at about 15 mb and is dominated by a well-defined, narrow but long (~3000 km) jet. The jet originates from an area to the northwest of the storm, extending in a clockwise direction to the southwest. The angular momentum budget shows that the horizontal eddy momentum flux, mostly representing the effect of the jet, is as important as the mean flux, indicating the dominance of the jet in the outflow layer. These characteristics of the outflow are in agreement with

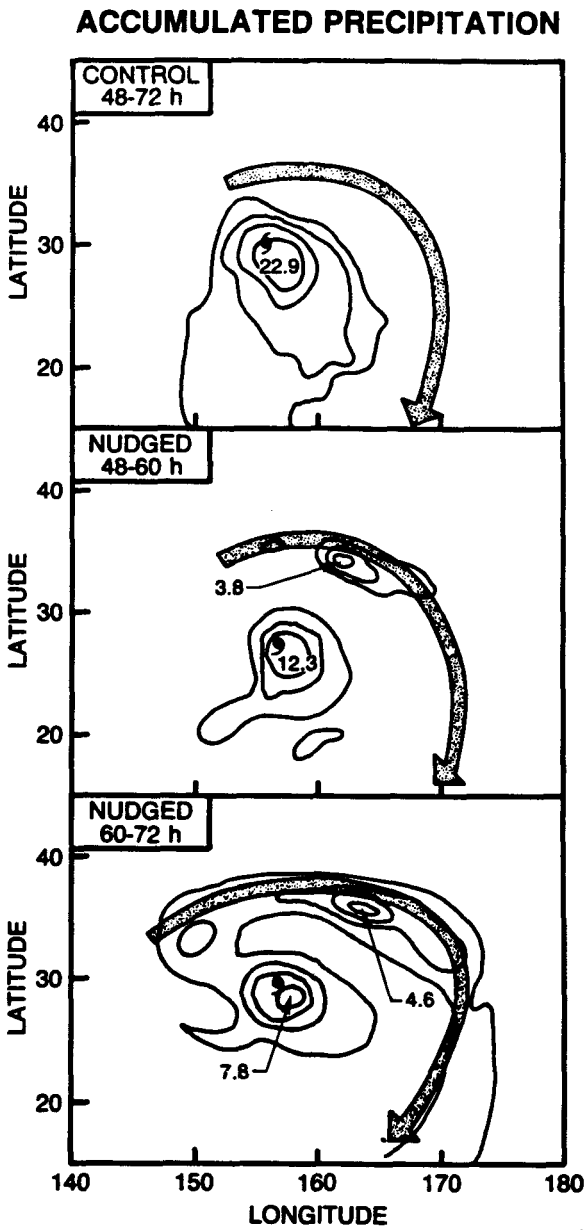

FIG. 12. The location of the outflow jet and distributions of a 24 h period accumulated precipitation for the control (upper panel) and two 12 h periods accumulated precipitation of Expt. 2.

observational studies (Palmen and Riehl 1957; Pfeffer 1958; Black and Anthes 1971).

Cross-sectional analyses of the outflow jet show the existence of a thermally direct secondary circulation around the jet in the jet entrance region and a thermally indirect one in the exit region. The thermally direct secondary circulation has an ascending branch on the anticyclonic shear side of the jet (i.e., closer to the cyclone center). The thermally indirect secondary circulation, on the other hand, has ascending motion on the cyclonic shear side. The secondary circulations have pronounced effects on the relative humidity and potential vorticity fields at the outflow levels. We found that a more intense tropical cyclone has a stronger outflow jet accompanied by a stronger circum-jet secondary circulation.

In an attempt to study the effect of upper tropospheric forcings on the structure and behavior of the model tropical cyclone, two variational numerical experiments were conducted. In Experiment 1, the total wind in the upper levels of the tropical cyclone within the radius of 5° lat is accelerated to simulate the possible consequence of superposing an upper tropospheric divergence or increasing the angular momentum influx over the tropical cyclone. In this case, the model tropical cyclone deepens by ~10 mb in 24 hours. These results suggest that the superposition of an upper tropospheric ridge over a tropical cyclone is a favorable condition for the intensification of a mature tropical cyclone. It is also evident that the convection plays an important role in linking the upper levels of the tropical cyclone to the lower troposphere.

In the second experiment, the region of the outflow jet with wind speeds greater than 20 m s^{-1} and between the radii of 5°–10° latitude from the storm center is forced to accelerate to simulate the possible effect of the confluence of the outflow jet with a westerly jet. The results from this experiment show that the convection is produced in the areas of the ascending branch of the secondary circulation. The convection away from the inner core in our simulation is competitive with the inner core convection and can weaken the tropical cyclone.

These results support the thesis of Holland and Merrill (1984) that tropical cyclones are susceptible to upper level forcings. As discussed earlier, the forcing of a certain region of the simulated tropical cyclone in our numerical experiments may not realistically reproduce the interaction between real tropical cyclones and the environment. To remedy this, a case study on the interaction between an observed tropical cyclone and upper-tropospheric systems is currently in progress and the results will be reported in the future.

Acknowledgments. We thank Mr. Edward Rodgers of GSFC/NASA, Dr. Rao Madala of NRL and Dr. Keith Sashegyi of SAIC for many beneficial discussions. We also thank Dr. Mark DeMaria of HRD/AOML/NOAA and Dr. John Molinari of SUNY at Albany for commenting on the manuscript. The work is supported by the Basic Research Program of the Naval Research Laboratory (NRL), a NRL Cray Computation Grant, the Tropical Cyclone Motion Initiative of the Office of Naval Research to NRL, and a NASA grant to NRL Contract S-56314-D. The first and third authors are supported by NRL Grant N00014-89-C-2234.

REFERENCES

Alaka, M. A., 1961: The occurrence of anomalous winds and their significance. *Mon. Wea. Rev.*, **89**, 482–494.

——, 1962: On the occurrence of dynamic instability in incipient and developing hurricanes. National Hurricanes Research Projects, Rep. No. 50, U.S. Weather Bureau, Washington, DC, 51–56.

Anthes, R. A., 1972: Development of asymmetries in a three-dimensional numerical model of the tropical cyclone. *Mon. Wea. Rev.*, **100**, 461–476.

——, 1974: The dynamics and energetics of mature tropical cyclones. *Reviews of Geophysics and Space Physics*, Vol. 12, No. 3, 495–522.

Black, P. G., and R. A. Anthes, 1971: On the asymmetric structure of the tropical cyclone outflow layer. *J. Atmos. Sci.*, **28**, 1348–1366.

Challa, M., and R. Pfeffer, 1980: Effects of eddy fluxes of angular momentum on model hurrican development. *J. Atmos. Sci.*, **37**, 1603–1618.

——, and ——, 1989: The formation of Atlantic hurricanes from cloud clusters and depressions. *J. Atmos. Sci.*, submitted.

Chang, S., K. Brehme, R. Madala and K. Sashegyi, 1989: A numerical study of the East Coast Snowstorm of 10–12 February 1983. *Mon. Wea. Rev.*, **117**, 1768–1778.

Chen, L., and W. M. Gray, 1984: Global view of the upper level outflow: Patterns associated with tropical cyclone intensity changes during FGGE. *15th Tech. Conf. on Hurricanes and Tropical Meteorology*, Amer. Meteor. Soc., Miami.

Eliasen, A., 1952: Slow thermally or frictionally controlled meridional circulations in a circular vortex. *Astrophys. Norveg.*, **5**, 19–60.

Frank, W. M., 1977: The structure and energetics of the tropical cyclone, part I: Storm structure. *Mon. Wea. Rev.*, **105**, 1119–1135.

Gray, W. M., 1979: Hurricanes: Their formation, structure and likely role in the tropical circulation. *Meteorology over the Tropical Oceans*, D. B. Shaw, Ed., Roy Meteor. Soc., 155–218.

Holland, G. J., 1983: Angular momentum transports in tropical cyclones. *Quart. J. Roy. Meteor. Soc.*, **109**, 187–209.

——, and R. T. Merrill, 1984: On the dynamics of tropical cyclone structural changes, *Quart. J. Roy. Meteor. Soc.*, **110**, 723–745.

Hoskins, B. J., M. E. McIntyre and A. W. Robertson, 1985: On the use and significance of isentropic potential vorticity maps. *Quart. J. Roy. Meteor. Soc.*, **111**, 877–946.

Kuo, Y.-H., and R. Reed, 1988: Numerical simulation of an explosively deepening cyclone in the Eastern Pacific. *Mon. Wea. Rev.*, **115**, 2081–2105.

Madala, R. V., S. W. Chang, U. C. Mohanty, S. C. Madan, R. K. Paliwal, V. B. Sarin, T. Holt and S. Raman, 1987: Description of the Naval Research Laboratory limited area dynamical weather prediction model. NRL Tech. Rep. No. 5992, Washington, DC, 131 pp.

McBride, J. L., 1981: Observational analysis of tropical cyclones formation. Part I: Basic description of data sets. *J. Atmos. Sci.*, **38**, 1117–1131.

Merrill, R. T., 1984: Structure of the tropical cyclone outflow layer. *Proc., 15th Tech. Conf. on Hurricanes and Tropical Meteorology*, Amer. Meteor. Soc., Miami.

——, 1988a: Characteristics of the upper-tropospheric environmental flow around hurricanes, *J. Atmos. Sci.*, **45**, 1665–1677.

——, 1988b: Environmental influences on hurricane intensification. *J. Atmos. Sci.*, **45**, 1678–1687.

Miller, B. I., 1963: The three-dimensional wind structure around a tropical cyclone. National Hurricane Research Project, Rep. No. 15, 41 pp.

Molinari, J., and D. Vollaro, 1989: External influences on hurricane intensity. Part I: Outflow layer eddy momentum fluxes. *J. Atmos. Sci.*, **46**, 1093–1105.

Ooyama, K. V., 1987: Numerical experiments of study and transient jets with a simple model of the hurricane outflow layer. Preprints, *17th Conf. on Hurricanes and Tropical Meteorology*, Amer. Meteor. Soc., Miami.

Palmen, E., and H. Riehl, 1957: Budget of angular momentum and kinetic energy in tropical cyclones. *J. Meteor.*, **14**, 150–159.

——, and C. W. Newton, 1969: *Atmospheric Circulation Systems.* Academic Press, 603 pp.

Pfeffer, R. L., 1958: Concerning the mechanisms of hurricanes. *J. Meteor.*, **15**, 113–119.

Riehl, H., 1954: *Tropical Meteorology.* McGraw-Hill.

Rodgers, E. B., 1987: Evidence of upper-tropospheric influence on tropical cyclone intensity change using satellite observations. Preprint, *17th Conf. on Hurricanes and Tropical Meteorology*, Amer. Meteor. Soc., Miami.

——, J. Stout, J. Steranka and S. Chang, 1990: Tropical cyclone/upper-atmospheric interaction as inferred from satellite total ozone observation. *J. Appl. Meteor.*, **29**, 934–954.

Sadler, J. C., 1976: The role of the tropical upper-tropospheric trough in early season typhoon development. *Mon. Wea. Rev.*, **104**, 1266–1278.

——, 1978: Mid-season typhoon development and intensity changes and the tropical upper-troposheric trough. *Mon. Wea. Rev.*, **106**, 1137–1152.

Sheets, R. C., 1968: Some mean hurricane soundings. *J. Appl. Meteor.*, **8**, 134–146.

Steranka, J., E. B. Rodgers and R. C. Gentry, 1986: The relationship between satellite measured convection burst and tropical cycline intensification. *Mon. Wea. Rev.*, **114**, 1539–1546.

Uccellini, L. W., P. J. Kocin, R. A. Petersen, C. H. Wash and K. F. Brill, 1984: The President's day cyclone of 18–19 February 1979: Synoptic overview and analysis of the subsynoptic jet streak influencing the pre-cyclogenetic period. *Mon. Wea. Rev.*, **112**, 31–55.